THE ASTROPHYSICAL JOURNAL, 354:52–57, 1990 May 1


# THE CORRELATION OF X-RAY AND OPTICAL LUMINOSITIES OF EARLY-TYPE GALAXIES USING NEW DATA AND DISTANCES[1]

R. HANK DONNELLY, S. M. FABER, AND R. M. O'CONNELL
University of California Observatories/Lick Observatory Board of Studies in Astronomy and Astrophysics, University of California at Santa Cruz
*Received 1989 June 16; accepted 1989 October 30*

## ABSTRACT

Using new apparent magnitudes and new distances as determined from the $D_n$-$\sigma$ method, we have reexamined the correlation of X-ray to optical luminosities for E and S0 galaxies. The residuals about our least-squares fits decline significantly but are not removed altogether. All attempts to correlate the remaining residuals with other structural and spectral parameters have given negative results, suggesting that some other, as yet unidentified, factor plays a role in defining X-ray luminosity with respect to optical luminosity. $L_X$ versus $L_B$ also appears to be a useful secondary distance indicator for early-type galaxies.

*Subject headings:* galaxies: distances — galaxies: photometry — galaxies: X-rays

## I. INTRODUCTION

Several authors have studied the correlation between optical and X-ray luminosities of early-type galaxies (Forman, Jones, and Tucker 1985; Trinchieri, Fabbiano, and Canizares 1986; Canizares, Fabbiano, and Trinchieri 1987). A strong correlation, with slope greater than unity, is seen, but the scatter is large. The amount and origin of the scatter are potentially interesting clues to the production and heating of the X-ray gas.

Since the slope of the correlation is steeper than unity, the scatter might be caused in part by distance errors to individual galaxies. Distances in the above studies were estimated using radial velocities corrected by a standard Virgocentric infall model (Aaronson *et al.* 1982). A recent study has obtained new magnitudes and distances for elliptical galaxies using the $D_n$-$\sigma$ relation (Dressler *et al.* 1987*a*; Lynden-Bell *et al.* 1988; Faber *et al.* 1989, hereafter 7S). We test here whether the correlation of $L_X$ versus $L_B$ improves using these new data. We also test whether residual scatter in the relation correlates with other structural variables such as effective radius, surface brightness, "boxiness," and $Mg_2$ line strength.

## II. $L_X$ VERSUS $L_B$

Apparent X-ray luminosities have been taken from the summary table of Canizares, Fabbiano, and Trinchieri (1987, hereafter CFT), which is the largest homogeneous sample of normal ellipticals available. The luminosity of NGC 6876 was increased by a factor of 10 (a misprint corrected with the help of Giuseppina Fabbiano). Two sets of distances were compared: the original radial velocity distances corrected for Virgo infall as tabulated by CFT, and the new $D_n$-$\sigma$ distances from 7S. Both sets assign mean distances to galaxies in groups, but the group membership assignments differ for three galaxies. For optical luminosities, we have in both cases used the new $B_T$ magnitudes and Galactic absorptions from 7S. The data are summarized in Table 1. $H_0 = 50\ \mathrm{km\ s^{-1}\ Mpc^{-1}}$ is assumed.

The resulting $L_X - L_B$ relations are compared in Figures 1*a* and 1*b*. The 7S distances result in a clearly tighter distribution. Filled circles represent ellipticals which have direct 7S measurements. Open circles are S0s that lack direct 7S estimates but are members of groups that do. They are included to show that agreement is not degraded by a fully consistent application of the new distances. Altogether, 62 out of the original 81 CFT galaxies have direct or indirect 7S distances and are plotted in Figure 1.

To quantify the decrease in scatter, we calculate correlation coefficients and residuals about one- and two-coordinate least-squares fits, as summarized in Table 2. The rms residual,

$$\overline{\Delta \log L_X} \equiv \left\{ \frac{\sum [y_i - y(x_i)]^2}{N} \right\}^{1/2}, \quad (1)$$

is given to demonstrate the quality of the fit. The fits utilized only detected galaxies, omitting the upper limits shown by arrows in Figure 1. Fits using only Virgo Cluster galaxies are also included for comparison.

The improvement with 7S distances can be demonstrated via a galaxy-by-galaxy comparison of Figures 1*a* and 1*b*; the residual of nearly every galaxy improves. Quantitatively, $\overline{\Delta \log L_X}$ shrinks by 20% (Table 2) using the new distances. For example, in the one-coordinate fit of $L_X$ on $L_B$, the rms residual declines from 0.40 to 0.33 dex.

It should be noted that Figure 1 was constructed to illustrate the pure effect of *distance errors* alone on the $L_X - L_B$ correlation. The only difference between the two panels is the choice of distance—the basic optical and X-ray flux data are the same. However, compared to the original figure in CFT, *both* panels in Figure 1 show a considerably tighter correlation. For example, using the exact same set of galaxies as shown here, the rms residual with the CFT data is found to be 0.48 dex, compared to 0.40 dex from panel (a), and 0.33 dex in panel (b) (see Table 2). The added improvement over CFT is due to the use of better optical magnitudes and to the corrected X-ray flux for NGC 6876. Altogether, we can say that, of the total improvement from the original CFT analysis to ours, about half is due to the use of new distances and half is due to improvements in the optical and X-ray fluxes.

Although they are not our primary concern, the slopes in the above fits merit a brief discussion. We are interested in least-squares fits primarily as a means for exploring the tightness of the correlations through the size of the residuals. Since our aim is mainly comparative, we feel it is adequate to use simple least-squares fits, omitting the upper limits but taking care to

[1] UCO/Lick Observatory Bulletin No. 1153.

TABLE 1

NEW LUMINOSITIES AND DISTANCES FOR X-RAY GALAXIES

| Name | Group Number[a] | $d$(CFT)[b] (Mpc) | $d$(7S)[b] (Mpc) | log $(L_B/L_\odot)$[c] | log $L_X$[d] |
|---|---|---|---|---|---|
| NGC 315 ..... | 271 | 101.9 | 97.5 | 11.56 | 41.87 |
| NGC 584 ..... | 26 | 37.1 | 29.0 | 10.61 | 39.95 |
| NGC 720 ..... | ... | 33.2 | 39.6 | 10.92 | 41.21 |
| NGC 1172 ..... | 29 | 32.0 | 44.4 | 10.47 | <40.27 |
| NGC 1332 ..... | ... | 30.4 | 38.5 | 10.85 | 40.95 |
| NGC 1380 ..... | ... | 26.2 | 27.5 | 10.63 | 40.59 |
| NGC 1395 ..... | 32 | 30.4 | 38.5 | 10.99 | 41.09 |
| NGC 1400 ..... | 32 | 10.4 | 38.5 | 10.71 | <40.35 |
| NGC 1407 ..... | 32 | 30.4 | 38.5 | 11.13 | 41.32 |
| NGC 1533 ..... | ... | 19.8 | 23.4 | 10.27 | 39.91 |
| NGC 1574 ..... | ... | 19.8 | 23.4 | 10.47 | <40.18 |
| NGC 1600 ..... | 34 | 93.7 | 77.6 | 11.25 | 41.65 |
| NGC 2314 ..... | ... | 77.4 | 97.6 | 11.07 | <41.26 |
| NGC 2300 ..... | 246 | 46.7 | 62.5 | 11.09 | 41.35 |
| NGC 2563 ..... | ... | 92.8 | 113.4 | 11.17 | 41.75 |
| NGC 2685 ..... | ... | 24.9 | 29.6 | 10.39 | 40.05 |
| NGC 2693 ..... | 214 | 97.3 | 95.0 | 11.12 | <41.29 |
| NGC 2859 ..... | ... | 40.3 | 70.2 | 11.18 | <40.73 |
| NGC 2974 ..... | ... | 42.9 | 41.0 | 10.84 | 40.65 |
| NGC 3078 ..... | 219 | 50.1 | 50.1 | 10.81 | 41.02 |
| NGC 3115 ..... | ... | 10.1 | 19.7 | 10.80 | <39.94 |
| NGC 3258 ..... | 46 | 56.2 | 67.4 | 10.94 | 41.43 |
| NGC 3377 ..... | 57 | 17.5 | 16.6 | 10.17 | <39.84 |
| NGC 3379 ..... | 57 | 17.5 | 16.6 | 10.45 | <40.02 |
| NGC 3489 ..... | ... | 17.5 | 16.6 | 10.18 | <39.75 |
| NGC 3585 ..... | 285 | 38.7 | 22.8 | 10.69 | 39.85 |
| NGC 3607 ..... | 48 | 24.0 | 38.5 | 11.15 | 41.03 |
| NGC 3818 ..... | ... | 36.8 | 62.6 | 10.76 | <40.93 |
| NGC 3923 ..... | 52 | 37.7 | 30.6 | 10.96 | 40.82 |
| NGC 4105 ..... | 245 | 40.0 | 40.6 | 10.92 | 40.66 |
| NGC 4251 ..... | ... | 30.0 | 28.4 | 10.45 | 39.69 |
| NGC 4291 ..... | 98 | 42.9 | 58.5 | 10.76 | 41.46 |
| NGC 4365 ..... | 56 | 25.7 | 25.8 | 10.76 | 40.29 |
| NGC 4374 ..... | 56 | 25.7 | 25.8 | 10.96 | 40.79 |
| NGC 4382 ..... | ... | 25.7 | 25.8 | 10.97 | 40.45 |
| NGC 4406 ..... | 56 | 25.7 | 25.8 | 11.07 | 41.58 |
| NGC 4459 ..... | ... | 25.7 | 25.8 | 10.42 | 40.09 |
| NGC 4472 ..... | 56 | 25.7 | 25.8 | 11.29 | 41.72 |
| NGC 4473 ..... | 56 | 25.7 | 25.8 | 10.53 | 39.95 |
| NGC 4477 ..... | ... | 25.7 | 25.8 | 10.52 | 40.04 |
| NGC 4550 ..... | ... | 25.7 | 25.8 | 10.08 | <39.85 |
| NGC 4552 ..... | 56 | 25.7 | 25.8 | 10.68 | 40.61 |
| NGC 4564 ..... | 56 | 25.7 | 25.8 | 10.23 | <39.84 |
| NGC 4589 ..... | 98 | 43.3 | 58.5 | 11.09 | 40.86 |
| NGC 4621 ..... | 56 | 25.7 | 25.8 | 10.75 | 39.96 |
| NGC 4636 ..... | 56 | 25.7 | 25.8 | 10.93 | 41.65 |
| NGC 4638 ..... | ... | 25.7 | 25.8 | 10.19 | 39.59 |
| NGC 4643 ..... | ... | 25.7 | 25.8 | 10.39 | 40.17 |
| NGC 4649 ..... | 56 | 25.7 | 25.8 | 11.11 | 41.40 |
| NGC 4665 ..... | ... | 25.7 | 25.8 | 10.44 | 39.91 |
| NGC 4697 ..... | ... | 25.7 | 15.4 | 10.55 | 39.82 |
| NGC 5077 ..... | 63 | 56.5 | 57.6 | 10.83 | 40.87 |
| IC 4296 ..... | 225 | 72.6 | 72.8 | 11.40 | 41.41 |
| NGC 5322 ..... | 254 | 46.8 | 32.1 | 10.77 | <40.60 |
| NGC 5485 ..... | 237 | 44.8 | 44.3 | 10.63 | <40.55 |
| NGC 5846 ..... | 70 | 40.6 | 45.1 | 11.23 | 41.94 |
| NGC 5898 ..... | 71 | 42.1 | 47.5 | 10.78 | 40.63 |
| NGC 6876 ..... | 269 | 79.0 | 57.1 | 11.20 | 41.26 |
| IC 1459 ..... | 231 | 27.5 | 43.0 | 11.11 | 40.86 |
| NGC 7562 ..... | 87 | 72.2 | 69.2 | 10.94 | 41.06 |
| NGC 7619 ..... | 87 | 69.8 | 69.2 | 11.07 | 41.61 |
| NGC 7626 ..... | 87 | 69.8 | 69.2 | 11.08 | 41.29 |

[a] Group number from Lynden-Bell *et al.* 1988.

[b] Distances from CFT and 7S, assuming $H_0 = 50\ \mathrm{km\ s^{-1}\ Mpc^{-1}}$.

[c] Optical luminosity using Galactic absorption and $K$-corrected magnitudes from Faber *et al.* 1989 and the 7S distances in col. (4). $M_B(\odot) = 5.48$ mag.

[d] X-ray luminosity in ergs $s^{-1}$ using apparent X-ray fluxes as tabulated by CFT and the 7S distances in col. (4). The X-ray luminosity of NGC 6876 (a misprint in CFT) has been increased by a factor of 10. " < " indicate upper limits.

use the same galaxies in all fits. However, we note that, upon going to the improved data and distances, the fits do tend to steepen somewhat as well as tighten. For example, using the same subset of galaxies described in the paragraph above, we find for the original CFT data a one-coordinate slope of $1.49 \pm 0.18$, which increases to $1.88 \pm 0.16$ with the new data and distances.

To decide on a best slope, we must confront the additional issue of whether a one- or two-coordinate fit is preferable. As we show below, the remaining residuals cannot be completely accounted for via observational errors, suggesting the probable existence of some hidden variable or variables. Lacking any conclusive theory for the origin of the scatter, we cannot ascribe it primarily to errors in either $L_X$ or $L_B$, and thus we cannot defend a fit of one coordinate on the other as being "superior." It therefore seems most conservative to favor a mean fit that is the average of $L_X$ on $L_B$ and vice versa. This is our "Two-Coordinate" fit in Table 2, for which we find a slope of $2.18 \pm 0.20$. This is steeper than the best CFT estimate of 1.73, which used a fit of $L_X$ on $L_B$ only. Inclusion of the upper limits in our analysis would not affect this result greatly but would probably steepen the slope still further. To summarize: the exponent of $L_X$ on $L_B$ may be slightly steeper than previous estimates and is probably somewhere in the range 1.9 to 2.2. This value cannot be improved further without a better understanding of the residuals, to which we now turn.

### III. THE RESIDUAL SCATTER

As noted above, the new distances reduce the scatter but do not completely eliminate it. The rms observational error contributions to $\Delta \log L_X$ are estimated as follows: 0.16 dex from errors in $B_T$ (7S); $\leq 0.1$ dex from errors in the X-ray fluxes (error bars in Forman, Jones, and Tucker 1985), and 0.17 dex from errors in the $D_n$-$\sigma$ distances (this is an average over all galaxies, taking group memberships into account and assuming an error of 21% per galaxy). The sum of these in quadrature is only 0.25 dex (0.20 dex for Virgo), which is considerably smaller than the observed scatter of 0.33–0.35 dex in Table 2. Some component of the residual scatter is therefore probably intrinsic. Further evidence for intrinsic scatter is the well-known pair in Virgo, NGC 4374–NGC 4406, whose optical luminosities are similar, but whose X-ray luminosities differ by a factor of 6; this is larger than any plausible measurement errors.

Correlation of the X-ray residuals with other parameters could provide an important clue to the origin of the X-ray emission. Moreover, it is now known that ellipticals are a two-dimensional manifold in their basic structural parameters (Dressler *et al.* 1987*b*; Djorgovski and Davis 1987), i.e., they populate a "fundamental plane" in $(R_e, \sigma, I_0)$-space. At constant $L_B$, there is a range in galaxy radius, with concomitant changes in surface brightness and velocity dispersion as expected for self-gravitating bodies in dynamical equilibrium (Faber *et al.* 1987).

It is therefore natural to ask whether the residuals in $L_X$ correlate with the size variations seen at constant $L_B$. To test this, we fit effective radius (from 7S) versus $L_B$ in Figure 2*a* and plot the residuals, $\Delta \log R_e$, versus $\Delta \log L_X$ in Figure 2*b*. No correlation is seen; variations in X-ray luminosity are evidently *not* related to variations in galaxy size at fixed $L_B$. All other similar tests were also negative; no correlation was found with $\Delta I_0(L_B)$, $\Delta\sigma(L_B)$, $\mathrm{Mg}_2$, $\Delta \mathrm{Mg}_2(\sigma)$, $\Delta D_n(\sigma)$, ellipticity, or 7S envelope type. To test further for a hidden parameter, we carried out a multidimensional least-squares fit of $L_X$ versus all

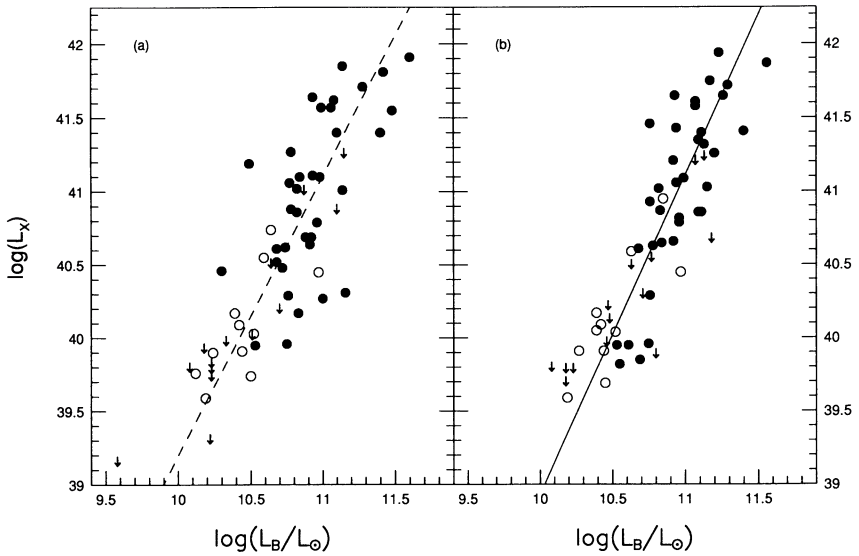


FIG. 1.—X-ray luminosity vs. blue luminosity for a subsample of galaxies from Canizares, Fabbiano, and Trinchieri (1987), using blue magnitudes from Faber *et al.* (1989). (*a*) Distances are those from CFT, using their groups and a Virgocentric infall model. (*b*) Distances are those from 7S, determined from the $D_n$-$\sigma$ method. Filled circles represent ellipticals for which complete data are available; open circles represent S0s for which a 7S distance was assigned based on cluster membership; arrows indicate upper limits, which were not used in the fits in Table 2. Slopes shown are two-coordinate fits.

available parameters from 7S. No reduction in residuals was seen beyond that expected from random chance. As a final test, we looked for a correlation between $L_X$ residuals and $(v/\sigma)_*$ from Davies *et al.* (1983) and isophote "boxiness" from Bender, Döbereiner, and Möllenhoff (1988) and Bender *et al.* (1989). We present plots of these tests in Figures 3*a*–3*c*. Again, no significant correlations were found.

While this work was being completed, we received a paper entitled "X-ray and Optical Properties of Elliptical Galaxies" by Djorgovski and de Carvalho (1989, hereafter DDC). In it, the authors point out a new correlation of $L_X$ with velocity dispersion and surface brightness. For the 7S data, they find

$$L_X \sim \sigma^{3.69} I_0^{-1.12} + \text{const} . \quad (2)$$

We believe that this result can be understood as essentially a restatement of the basic $L_X - L_B$ correlation. Making use of the equation of the fundamental plane (Faber *et al.* 1977),

$$R_e \sim \sigma^{1.35} I_0^{-0.84} , \quad (3)$$

plus the basic relation

$$L_B \sim I_0 R_e^2 , \quad (4)$$

we can recast equation (2) as

$$L_X \sim L_B^{1.45} \sigma^{-0.22} I_0^{-0.13} , \quad (5)$$

which is seen to depend mainly on $L_B$ and only weakly on $\sigma$ and $I_0$. Furthermore, the mean residual $\Delta \log L_X$ about equation (2) is 0.36 dex, which is slightly larger than the 0.33–0.35 dex of $L_X$ on $L_B$ alone. Thus, the introduction of the new variables $\sigma$ and $I_0$ does not appear to offer any significant improvement. The fact that equation (5) looks slightly different from the fits in Table 2 can be ascribed to uncertainty and scatter in the observed structural relations and in $L_X$ versus $L_B$.[2]

[2] Note that the slopes in eq. (2) were found by DDC using CFT distances for the $L_X$ luminosities. We have redone their fit using the new 7S distances and find $L_X \sim \sigma^{3.69} I_0^{-1.23}$, which is hardly changed from their result. The residuals in $\Delta \log L_X$ are also essentially unchanged.

TABLE 2

FITS OF $L_X$ VERSUS $L_B$

| DATA GROUP | NUMBER OF POINTS | CORRELATION COEFFICIENT | TWO-COORDINATE FIT[a] | | Y-FIT ONLY[b] | |
|---|---|---|---|---|---|---|
| | | | Slope | $\Delta \log L_X$[c] (dex) | Slope | $\Delta \log L_X$[c] (dex) |
| CFT[d] ..... | 47 | 0.78 | $1.91 \pm 0.26$ | 0.421 | $1.49 \pm 0.18$ | 0.397 |
| 7S[d]: | | | | | | |
| All ..... | 47 | 0.86 | $2.18 \pm 0.20$ | 0.346 | $1.88 \pm 0.16$ | 0.334 |
| Virgo ..... | 16 | 0.87 | $2.31 \pm 0.22$ | 0.350 | $2.01 \pm 0.18$ | 0.338 |

[a] Mean of least-squares fits of $\log L_X$ on $\log L_B$ and $\log L_B$ on $\log L_X$, as follows: data were translated and scaled to have zero mean and RMS $\sigma = 1$ in each coordinate. Standard regression lines were then fit. Mean regression was taken to bisect the angles of $\log L_X$ on $\log L_B$ and vice versa in the scaled coordinate system. The slope shown is that obtained when original coordinate scales are recovered. Galaxies with upper limits in Fig. 1 were not used.

[b] Standard least-squares regression of $\log L_X$ on $\log L_B$.

[c] RMS residuals of $\log L_X$.

[d] CFT: radial velocity distances corrected for Virgocentric infall as tabulated by CFT. 7S: distances based upon $D_n - \sigma$ relation as tabulated by Faber *et al.* 1989. All fits use new magnitudes from Faber *et al.* 1989 and the corrected X-ray flux for NGC 6876.

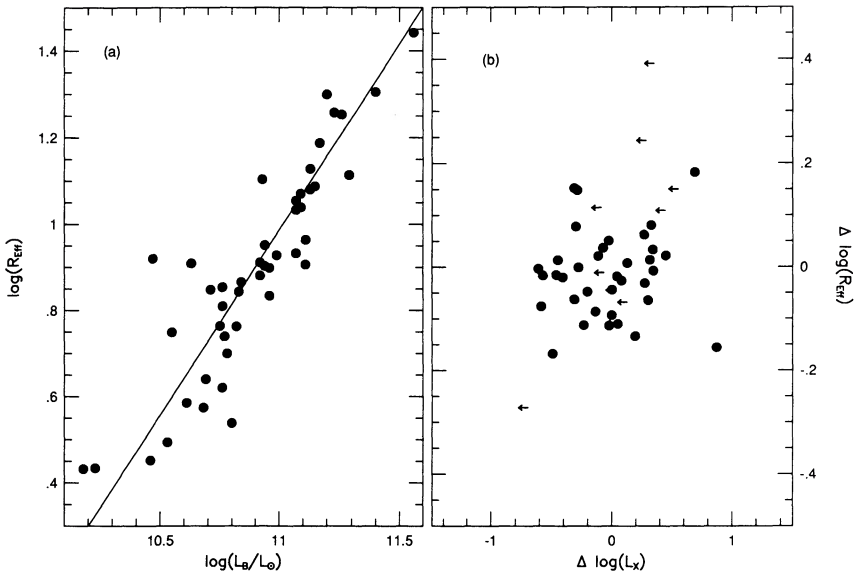


FIG. 2.—Example of typical results of test for correlation of residuals in $L_X$ with other parameters, such as effective radius, velocity dispersion, surface brightness, $Mg_2$, etc. (*a*) Effective radius vs. blue luminosity. (*b*) Residual in effective radius as compared to residual in X-ray luminosity. Structural data were taken from Faber *et al.* (1989). Arrows indicate galaxies for which the X-ray luminosity is only an upper limit. This, and all similar plots using different parameters, shows no correlation.

DDC also explore trends with boxiness, color gradients, and $(v/\sigma)_*$. They find positive correlations with $L_X$, which they consider to be evidence for increased X-ray emission due to mergers. This at first sight seems to contradict our negative results above for two of the same three parameters. The discrepancy can be explained, however, by noting that boxiness and $(v/\sigma)_*$ are in turn both correlated with $L_B$ (Bender, Döbereiner, and Möllenhoff 1988; Davies *et al.* 1983). The new correlations are thus again the original $L_X - L_B$ correlation restated. The real test of a new parameter ought to be whether or not it can reduce the $\Delta$ log $L_X$ residuals, and, as we have seen, neither boxiness nor $(v/\sigma)_*$ has any noticeable effect on that.

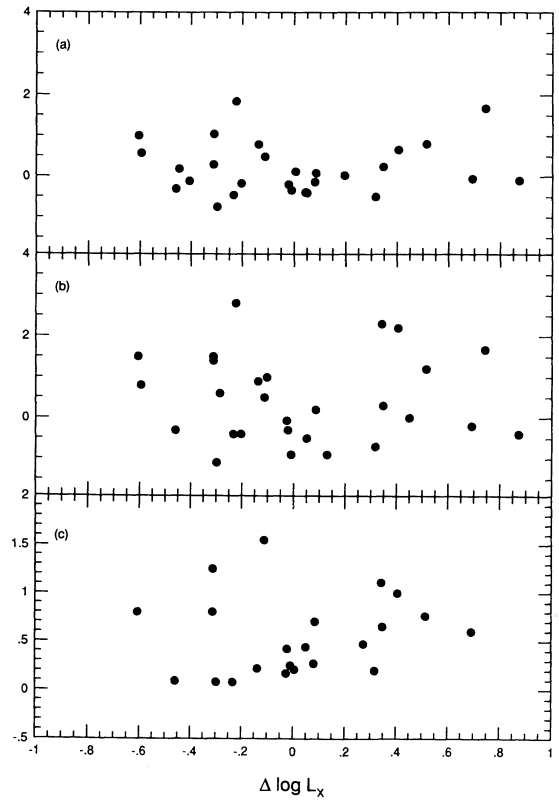


FIG. 3.—Plots of $\Delta$ log $L_X$ vs. isophote "boxiness" and rotation velocity. (*a*) Average values of $a_4$ within 30″ from Bender, Döbereiner, and Möllenhoff (1988). (*b*) Peak values of $a_4$ from Bender *et al.* (1989). (*c*) Dimensionless rotation $(v/\sigma)_*$ from Davies *et al.* (1983). No correlations are seen.

## IV. THEORIES FOR THE X-RAY EMISSION

These results can be compared to theoretical models for the X-ray emission. There are two limiting cases for steady state models in which the bolometric X-ray correction and the enthalpy fluxes at the boundary and origin can be ignored (Loewenstein and Mathews 1987; Sarazin and White 1988). In the first case, the dominant mechanism for heating the X-ray gas is supernovae, the number of which should simply scale with the optical luminosity. In this case,

$$L_X \sim L_B \,. \tag{6}$$

In the other limit, the dominant energy source comes from gravitational compression, which scales with the depth of the potential well. In this mode,

$$L_X \sim L_B \sigma^2 \sim L_B^{1.5} \,. \tag{7}$$

A point of comparison is the observed slopes in Table 2 versus these predicted slopes. As a group, the fitted slopes are steeper than predicted by the models, and the discrepancy is largest for the slope that we consider best: the two-coordinate fit using 7S distances, which yields an exponent of $2.18 \pm 0.20$ (2.31 for Virgo only). To see explicitly whether inclusion of $\sigma$ improves the residuals, as suggested by equation (7), we also fit $L_X$ on $L_B$ plus $\sigma$. As expected from our previous multiparameter fits, no improvement was seen.

Equations (6) and (7) are simplifications and do not represent the behavior of real steady state models very well (Sarazin and White 1988)—let alone time-evolving models, which are too complex to parameterize easily (Lowenstein and

Mathews 1987; D'Ercole *et al.* 1989). Actual models fit the data somewhat better than equations (6) and (7), but the detailed assumptions still leave much to be desired. For example, models for galaxies of different mass have been computed, but the structural parameters (including $M/L$) have not yet been varied in such a way as to explore the full two-dimensional manifold for ellipticals in a completely realistic and self-consistent way.

Another interesting parameter is the Hubble constant. Up to now, essentially all models have assumed $H_0 = 50$. A change in $H_0$ not only alters the zero point of the observational locus (Fig. 1), it also enters the models in several ways. $H_0$ sets the zero point of the mass-to-light ratio scale and hence the depth of the potential well for a given galaxy luminosity. It affects the assumed luminosity per supernova and the specific supernova rate per unit luminosity as deduced from supernovae counts. Finally, it strongly influences the mass and luminosity densities of galaxies through their measured radii. These changes, as it turns out, do not affect the relative locations of models and data for the steady state cases in equations (6) and (7), because model and data move together in these situations. However, nonequilibrium evolving models could well be affected by a change in $H_0$. Realistic computer simulations are needed to tell for sure.

Finally, we note that the new data (distances, optical and X-ray fluxes) seem to have altered the basic morphology of the $L_X - L_B$ relation. Previously, in CFT, it appeared that the region occupied by the galaxies was a parallelogram, with top and bottom sides parallel to $L_X \sim L_B$. D'Ercole *et al.* (1989) interpreted these boundaries as the limiting cases $L_X = L_{\rm discrete}$ and $L_X = L_{\rm SN}$, with luminosity provided entirely by discrete sources and by supernovae, respectively. Galaxies between these loci represented objects with varying amounts of interstellar medium and densities of outflowing wind. Since the amount of interstellar medium might plausibly be sensitive to several model parameters, both structural and environmental, the wide range of X-ray fluxes in the intermediate region was potentially explained.

This interpretation might still be fundamentally correct. However, the reduced scatter in $L_X$ indicates a greater degree of regularity than was previously suspected. Indeed, in this picture, the steep slope *itself* now represents the transition between empty galaxies (small ones) and full galaxies (large ones). Our unsuccessful search above has eliminated the most obvious structural parameters, beyond $L_B$ itself, that could modulate $L_X$ between $L_{\rm discrete}$ and $L_{\rm SN}$.

## V. A NEW DISTANCE INDICATOR FOR EARLY-TYPE GALAXIES

Thus far, we have assumed that the $D_n$-$\sigma$ distances are a genuine improvement over the old ones and that reductions in the $L_X - L_B$ residuals are real. However, the new distances also carry with them the implication of a large-scale flow of galaxies (Lynden-Bell *et al.* 1988) that is troubling to conventional cosmological models. Thus, alternative interpretations should be carefully considered. One such is the suggestion (Djorgovski, DeCarvalho, and Han 1989; Silk 1989) that the zero point of the $D_n$-$\sigma$ relation varies spatially in such a way as to *mimic* a large-scale flow. This could happen most easily through changes in $M/L$ of the luminous portions of elliptical galaxies, for example, via changes in the luminosity of the stellar population at fixed galaxy mass (Faber *et al.* 1987).

Arguments and evidence have been given elsewhere against this interpretation (Burstein, Faber, and Dressler 1989). The X-ray data here afford an independent check, albeit one that must be used carefully. It is not correct simply to point to the tightening of the $L_X - L_B$ relation as conclusive proof of the superiority of the new distances, for this ignores the possibility that systematic errors in $D_n$-$\sigma$ might be accompanied by *corresponding* systematic deviations in $L_X - L_B$. Thus, we may have used erroneous distances from $D_n$-$\sigma$ to "clean up" illusory distance errors in $L_X - L_B$.

From a sample consisting purely of field galaxies, it is impossible to disentangle the two choices without further information. Fortunately, however, the present X-ray sample contains nine cluster galaxies in Virgo and three more in Pegasus. For these groups, whose galaxies are known to be at a common distance, it is possible to compare residuals in the two relations measured relative to the *cluster* zero points. Here we are comparing residuals in the cluster $D_n$-$\sigma$ relation with residuals in $L_X - L_B$ on a galaxy-by-galaxy basis. Such a plot shows no correlation. Hence, there is no evidence, so far, for any correlated systematic errors in $D_n$-$\sigma$ and $L_X - L_B$. It seems promising, therefore, that $L_X - L_B$ does in fact provide an independent corroboration of $D_n$-$\sigma$. More cluster galaxies would help to establish this fact with greater certainty.

From the scatter in Figure 1, we can estimate the rms error of the $L_X - L_B$ relation when used as a distance indicator. The error, $\Delta \ln R$, is 0.39, compared to 0.21 for $D_n$-$\sigma$ and $\leq 0.16$ for Tully-Fisher (Lynden-Bell *et al.* 1988; Faber and Burstein 1989). In terms of raw accuracy, then, the new method is not very competitive. However, for groups it offers an important independent check on other methods. For example, it would be useful to apply the method to the Hydra-Centaurus groups that show large velocities when studied with $D_n$-$\sigma$ (Lynden-Bell *et al.* 1988). Djorgovski and de Carvalho have also noted that $L_X - L_B$ (and $L_X - \sigma - I_0$) are useful distance indicators.

## VI. CONCLUSIONS

Our analysis has shown that the $L_X - L_B$ relation improves when new data and $D_n$-$\sigma$ distances are used. Real scatter still remains in $L_X$, but it does not seem to correlate with any other structural parameter. The slope of $L_X$ versus $L_B$ is slightly steeper than before, and the relation now looks more like a true power law rather than a filled parallelogram. $L_X - L_B$ promises to be a useful secondary distance indicator for early-type galaxies; it independently provides support for the $D_n$-$\sigma$ method.

We would like to thank William G. Mathews and an anonymous referee for comments that substantially improved this paper. This research was supported by NSF grant AST 87-02899.

## REFERENCES

Aaronson, M., Huchra, J., Mould, J., Schechter, P., and Tully, B. 1982, *Ap. J.*, **258**, 64.
Bender, R., Döbereiner, S., and Möllenhoff, C. 1988, *Astr. Ap. Suppl.*, **74**, 385.
Bender, R., Surma, P., Döbereiner, S., Möllenhoff, C., and Madjesky, R. 1989, *Astr. Ap.*, **217**, 35.
Burstein, D., Davies, R. L., Dressler, A., Faber, S. M., Stone, R. P. S., Lynden-Bell, D., Terlevich, R. J., and Wegner, G. 1987, *Ap. J. Suppl.*, **64**, 601.
Burstein, D., Faber, S. M., and Dressler, A. 1989, *Ap. J.*, submitted.
Canizares, C. R., Fabbiano, G., and Trinchieri, G. 1987, *Ap. J.*, **312**, 503.
Davies, R. L., Efstathiou, G., Fall, S. M., Illingworth, G., and Schechter, P. L. 1983, *Ap. J.*, **266**, 41.
D'Ercole, A., Renzini, A., Ciotti, L., and Pellegrini, S. 1989, *Ap. J. (Letters)*, **341**, L9.
Djorgovski, S., and Davis, M. 1987, *Ap. J.*, **313**, 59.

Djorgovski, S., and DeCarvalho, F. 1989, preprint.
Djorgovski, S., DeCarvalho, R., and Han, M.-S. 1989, in *The Extragalactic Distance Scale*, ed. S. van den Burgh and C. J. Pritchet (Provo: Brigham Young University Print Services), p. 329.
Dressler, A., Faber, S. M., Burstein, D., Davies, R. L., Lynden-Bell, D., Terlevich, R. J., and Wegner, G. 1987*a*, *Ap. J. (Letters)*, **313**, L37.
Dressler, A., Lynden-Bell, D., Burstein, D., Davies, R. L., Faber, S. M., Terlevich, R. J., and Wegner, G. 1987*b*, *Ap. J.*, **313**, 42.
Faber, S. M., and Burstein, D. 1989, in *Large-Scale Motions in the Universe*, ed. V. C. Rubin and G. V. Coyne (Princeton: Princeton University Press), p. 115.
Faber, S. M., Burstein, D., Davies, R. L., Dressler, A., Lynden-Bell, D., Terlevich, R. J., and Wegner, G. 1987, in *Nearly Normal Galaxies*, ed. S. M. Faber (New York: Springer-Verlag), p. 175.
Faber, S. M., Wegner, G., Burstein, D., Davies, R. L., Dressler, A., Lynden-Bell, D., and Terlevich, R. J. 1989, *Ap. J. Suppl.*, **69**, 763.
Forman, W., Jones, C., and Tucker, W. 1985, *Ap. J.*, **293**, 102.
Loewenstein, M., and Mathews, W. G. 1987, *Ap. J.*, **319**, 614.
Lynden-Bell, D., Faber, S. M., Burstein, D., Davies, R. L., Dressler, A., Terlevich, R. J., and Wegner, G. 1988, *Ap. J.*, **326**, 19.
Sarazin, C. L., and White, R. E. 1988, *Ap. J.*, **331**, 102.
Silk, J. 1989, preprint.
Trinchieri, G., Fabbiano, G., and Canizares, C. R. 1986, *Ap. J.*, **310**, 637.

R. HANK DONNELLY and S. M. FABER: University of California Observatories, Lick Observatory, University of California, Santa Cruz, CA 95064

R. M. O'CONNELL: Department of Astronomy, College of the Redwoods, Eureka, CA 95501